Theor Chim Acta (1996) 93: 177–189

Theoretica Chimica Acta

Effect of crystal potential on dynamic polarizability of negative ions

D. Ray, P.C. Schmidt, Alarich Weiss

Institut für Physikalische Chemie, Technische Hochschule Darmstadt, Petersenstraße 20, D-64287 Darmstadt, Germany

Received May 4, 1995/Final revision received July 6, 1995/Accepted August 11, 1995

Summary. We combine a time-dependent approach with a crystal potential model to study environment-specific optical linear response of closed-shell ions within crystals under the influence of an external time-varying field. It is shown how the dynamic dipole polarizability of free halogen anions within the normal dispersion region is altered due to the crystal potentials felt by the anions in environments appropriate for different binary cubic ionic lattices. The pole-positions of the in-crystal anion polarizability are found to be consistent with the vacuum ultraviolet absorption edges of the corresponding alkali halides and to vary linearly with the lattice potentials at the anion sites in these salts. It is observed that the crystal potential induces quite a large enhancement in the anionic absorption oscillator strengths of these dipole transitions, thereby making these values conform well with those of the first excitonic absorptions in such crystals.

Key words: Crystal potential – Dynamic polarizability – Absorption oscillator strength – Halogen anion

1 Introduction

The response behaviour of free or isolated ions to external fields is recognised as a subject of vast intrinsic interest. The presence of a crystalline environment modifies such "gas phase" response of ions considerably, and a reasonable amount of theoretical effort [1–17] has been directed over the years towards modelling and analyzing the influence of environments on ionic response and related properties (the electronic polarizability of an ion, for instance) by means of *ab initio* quantum chemical approaches. The central problem in these studies is the construction of an appropriate crystalline environment and a prototype central ion and to compute the consequent modification of the free ion wavefunction, which (together with the external field-perturbed one) is required for determining ionic response properties of the applied field. The basic feature present in these calculations are,

(i) the solid is taken to be fully ionic, so that the straightforward addivity rule for the individual anionic and cationic in-crystal polarizability is valid within a

formula unit; the sum may then be used in modelling response-related other macroscopic quantities (like the high-frequency dielectric constant or the index of refraction) of the solid via the well-known Clausius–Mossoti relation, on the assumption that every ion participates in the process.
(ii) No explicit consideration of the full crystal with three-dimensional translational invariance resulting in periodic boundary condition imposed on the lattice potential and the crystal wavefunction (the Bloch states) is incorporated. Instead, a spherically-symmetric analytic model of the crystal potential [1–6] similar to the one originally used by Watson [18] to stabilize the O^{2-} ion in crystals, or, spherically-averaged sum of pseudopotentials [7] was adopted for approximating the effect of environments on the single ion in question. At a somewhat more sophisticated level [8–17], the central ion at the local site of full cubic symmetry in certain ionic crystals was taken with or without the surrounding nearest-neighbour cluster embedded in a finite-fragment point-charge representation of the remainder of the crystal.
(iii) Most of the calculations [1–15] have dealt with the time-independent or stationary response and related static properties of ions induced by a steady external electric field. Dynamic in-crystal response at imaginary frequencies has been studied using time-dependent perturbation theory for obtaining the long-range dispersion coefficients for ion pairs and triples of the inert-gas structures [16, 17].

In the present communication we have extended our study to include the effect of a time-varying external field and the influence of different ionic environments on frequency (real)-dependent polarizability of ions via the combination of a time-dependent procedure with the model crystal potential approach. The dynamic in-crystal response of ions is intimately connected to the optical dispersion phenomena associated with high-frequency absorptions in solids. However, within our approach, the interband transitions in solids cannot be reached since the model does not take account of the periodic aggregate of ions. On the other hand, the current method is expected to reproduce the localised electronic excitations at the ion sites within crystals, as shall be evident in the last section of our report. In this calculation we restrict ourselves to a Madelung-energy-dependent, variable-radius Watson sphere model of the crystal potential. Quite reasonable quantitative prediction of static response properties could be possible using this model in earlier calculations [4, 6]. Additionally, the numerical ease offered by this model is considerable – the response property computation for ions within crystals is no more complicated than that for a free ion. We have not included the effects of electron correlation and spin–orbit interaction in our study and have worked out following the coupled Hartree–Fock (CHF) scheme embodied within a time-dependent perturbation-variation theory (TDPVT) framework. Some of the closed-shell halogen anions and alkali-metal cations of the s^2- and p^6-configurations both in their free-states and pertaining to well-known ionic crystal lattice constitute the systems for the present investigation. In the subsequent sections, we briefly enumerate the essential theoretical steps involved in our calculation and present a discussion of the results obtained for the systems under consideration.

2 Method

The unperturbed Hamiltonian H_0^C of the ion in a crystal potential (the superscript 'C' shall refer to crystals and we adopt the atomic units throughout unless specified

otherwise) is formally expressed as,

$$H_0^C = H^{Free} + V^C \tag{1}$$

where the free-ion Hamiltonian H^{Free} consists of the usual electronic kinetic energy, electron-nuclear attraction, and the interelectronic repulsion terms. The crystal field V^C at the ion site due to the surrounding lattice is assumed to be simulated by placing the ion in question (hereafter referred to as the "crystal-ion") at the center of a uniformly charged spherical shell of radius R, with the charge n being of equal magnitude and opposite sign to that of the ion enclosed. The potential generated by such a spherical shell is given by,

$$\begin{aligned} V^C(r) &= n/R \quad r \leqslant R \\ &= n/r \quad r > R \end{aligned} \tag{2}$$

where $n = -n_{ion}$. The radius R is chosen following the criterion: $V^C = V^{Madelung}$ (for $r < R$), such that the Madelung potential of the ionic crystal lattice is introduced at the probe ion site. Thus, the electrostatic point charge model of an ionic lattice and the geometry of a specific crystal structure are implicitly recognised while the short-range repulsive compression due to overlap between neighbouring lattice sites are ignored simultaneously in the current approach.

Now, the one-electron Hartree–Fock–Roothaan equations, containing the additional crystal potential term for crystal-ions, are solved self-consistently by the standard basis-set expansion method using Slater-type orbitals (STO) to obtain the single-particle orbitals (η_j^C) and the corresponding energies (ε_j^C). In this process, the total (unperturbed ground state) crystal-ion energy E_0^C is optimised simultaneously with respect to the expansion coefficients as well as the exponents of the basis functions following the conventional iterative procedure. The computer program of Pitzer [19] for free ions is appropriately modified for this purpose by introducing the crystal potential in the Fock operator.

At the next stage, we consider the dynamic response of the crystal-ion to an external spin-independent harmonic field treated as a time-dependent perturbation and represented by

$$H'(t) = \sum_j h_j(r)\exp(-i\omega t) + \text{complex conjugate} \tag{3}$$

where

$$h(r) \sim r^l Y_{l0}(\theta, \phi) \tag{4}$$

In this calculation we consider only the dipolar perturbation ($l = 1$) that admixes two-component first-order oscillatory corrections $\delta\eta_j^{C\pm}$ to each unperturbed (ground state) crystal-ion orbital η_j^C. These admixtures are subsequently determined variationally in two steps. First, we introduce the following time-dependent normalised functional [20–22] of the Dirac–Frenkel type averaged over the complete cycle of the applied field:

$$J(\Phi^C) = (1/T)\int_0^T \frac{\left\langle \Phi^C \middle| H^C - i\frac{\partial}{\partial t} \middle| \Phi^C \right\rangle dt}{\langle \Phi^C | \Phi^C \rangle dt} \tag{5}$$

which is subject to the optimisation condition

$$\delta J(\Phi^C) = 0 \tag{6}$$

where Φ^C stands for the total perturbed crystal-ion wavefunction corresponding to the perturbed crystal-ion Hamiltonian $H^C = H_0^C + H'$ in presence of the external field and is expressed by means of the normalised antisymmetriser A in the following manner (through first-order):

$$\Phi^C(t) = \exp(-iE_0^C t) A \prod_j (\eta_j^C + \delta\eta_j^{C-} e^{-i\omega t} + \delta\eta_j^{C+} e^{i\omega t}) \tag{7}$$

Thus we expand the radial part of the perturbed admixtures in a linear combination of suitable Slater-type bases where the coefficients of expansion are to be obtained following a linear variation procedure. And finally, with a knowledge of these two-dependent first-order admixtures, the linear response of the crystal-ion to the applied periodic field may be studied in terms of the dynamic dipole electronic polarizability (only the real part is considered here) as a function of the frequency of the external field:

$$\alpha_d(\omega) = \sum_j (\langle \delta\eta_j^{C-} | r\cos\theta | \eta_j^C \rangle + \langle \delta\eta_j^{C+} | r\cos\theta | \eta_i^C \rangle) \tag{8}$$

3 Results and discussion

Our system of interest is the halogen anion X^- ($\equiv F^-$ and Cl^-) in a set of crystal potentials corresponding to different alkali halides M^+X^- of the rock-salt (face-center-cubic) type, where M^+ represents the metal cations Li^+, Na^+, K^+, Rb^+ and Cs^+. Also considered are the cations Li^+, Na^+ and K^+ in their respective fluoride and chloride salts. All the positive and negative ions treated here are of the closed-shell configuration with spherically symmetric ground states in both their free and crystalline states, and this condition is maintained by the choice of the spherically symmetric model of the crystal potential in our calculation. Besides, the well-established idea of an environment-sensitive polarizability (i.e., crystal-dependent for a constituent ion) is also implied in our consideration of a Madelung-energy-dependent radius R of the potential sphere (see Eq. 2).

Under a dipole perturbation, the dipole polarizability α_d is made up of the following first-order perturbed orbital contributions: (1) the p-type polarization of the s-orbitals, (2) the s-type polarization of the p-orbitals and (3) the d-type polarization of the p-orbitals. Adequate representation of each of these polarization functions separately in terms of a quite large and flexible 15 parameter STO expansion is ensured on the basis of a very well-converged set of the corresponding orbital polarizabilities. In Table 1 we have summarized the calculated $\omega = 0$ limits of the total dipole polarizability of the ions in various crystalline environments together with a break-up of the valence-orbital contributions. The inner-shell contributions are always insignificant compared to these and are omitted, though they are counted in the total. For the sake of comparison we have also presented the results available from earlier static investigations. Fowler and Madden [9] performed their analysis for negative ions following two schemes: first, using a model environment where the central ion is surrounded by point charges on

Table 1. Static limits of the dipole polarizabilities (in a.u.) of anions and cations – in-crystal and vacuum (free) values

Ion	Environment	Static dipole polarizability					
		Present				Other results	
		Valence orbital contributions			Total	Theory	Empirical[a]
		$2s \rightarrow p$	$2p \rightarrow s$	$2p \rightarrow d$			
F^-	LiF	1.042	1.028	4.150	6.223	(7.30, 5.39)[b], 5.48[c]	5.99
	NaF	1.005	1.402	4.564	6.973	(8.29, 6.37)[b], 5.99[c], 6.97[d]	6.91
	KF	0.969	1.810	4.987	7.769	(9.20, –)[b], 7.72[d]	7.71
	RbF	0.956	1.995	5.190	8.144	(9.49, –)[b], 7.94[d]	7.96
	CsF	0.944	2.174	5.374	8.495	(9.78, –)[b]	8.23
	vacuum	0.890	3.228	6.436	10.556	10.65[b], 10.63[d]	
		$3s \rightarrow p$	$3p \rightarrow s$	$3p \rightarrow d$			
Cl^-	LiCl	2.867	2.475	14.640	20.003	(23.7, 18.9)[b], 19.0[c]	19.44
	NaCl	2.775	3.141	15.489	21.426	(26.7, 20.2)[b], 19.5[c], 20.16[d]	20.97
	KCl	2.661	4.001	16.521	23.207	(27.5, –)[b], 21.55[d]	22.54
	RbCl	2.617	4.343	16.913	23.897	(28.2, –)[b], 22.07[d]	23.09
	CsCl	2.551	4.900	17.545	25.021		
	vacuum	2.287	7.869	20.768	30.953	31.47[b], 29.50[d]	
		$1s \rightarrow p$					
Li^+	LiF	0.1901			0.190		
	LiCl	0.1895			0.190		
	vacuum	0.1894			0.189	0.189[b]	
		$2s \rightarrow p$	$2p \rightarrow s$	$2p \rightarrow d$			
Na^+	NaF	0.488	– 0.256	0.726	0.959	(0.945, –)[b], 0.992[d]	
	NaCl	0.488	– 0.259	0.720	0.950	0.985[d]	
	vacuum	0.488	– 0.261	0.719	0.948	0.944[b], 0.958[d]	
		$3s \rightarrow p$	$3p \rightarrow s$	$3p \rightarrow d$			
K^+	KF	1.610	– 0.568	4.576	5.627	(5.404, –)[b], 5.547[d]	
	KCl	1.618	– 0.617	4.504	5.512	5.453[d]	
	vacuum	1.616	– 0.628	4.482	5.477	5.399[b], 5.196[d]	

[a] Ref [23]
[b] Ref [9] (for crystal-ions, the 'CRYST' and 'CLUS' results respectively)
[c] Ref [15] ('CLUS' results)
[d] Ref [4] (NHF results including self-consistency)

a cubic lattice of 5^3 sites (referred to as 'CRYST'), and then with a more realistic model (called 'CLUS') in which the six nearest-neighbour cations were also considered with basis functions while the rest of the finite lattice was treated as point charges. Positive ions being much less sensitive to the crystalline environments, only the 'CRYST' results were given for them. Fowler and Madden estimated that the correlation correction increases the CRYST-anion polarizability over the CRYST-coupled Hartree–Fock (CHF) value by approximately 25% (in LiF) to 40% (in CSF) for F^-, and by about 5% (in LiCl) to 10% (in RbCl) for Cl^-. The CLUS-anion polarizability was seen to rise up due to electron correlation by about 15–20% for F^- and 2–4% for Cl^- over the corresponding CLUS-CHF values (for free F^- and Cl^- ions, these contributions are about 50% and 15% of the CHF values). We have not computed the correlation contribution within our model. In Table 1 we have quoted Fowler and Madden's results for the free and in-crystal ions obtained at the CHF level along with the numerical Hartree–Fock (NHF) results including the self-consistency effect of Schmidt et al. [4] using a variable radius spherical model of the crystal potential similar to this work. Empirical in-crystal anion polarizability values obtained by Coker [23] are also cited for comparison.

The large confinement effect of the crystalline environments on the anions is clearly seen in all these results including ours. As a result of increasing compression of the anionic charge-cloud by the lattice potential as the interionic distance reduces in smaller halides, the anion becomes more tightly bound and hence less polarizable in a free to crystal transition. On the contrary, a very small expansion of the cation in the lattice potential leads to an almost negligible increase in its polarizability which is also supported by our calculation. Assuming the validity of the addivity rule for environment-specific polarizability of the anion and cation in ionic crystals, we have obtained the in-crystal pair polarizabilities in a few alkali halides. In Table 2 these are compared with the values recommended in the earlier critical compilation of Wilson and Curtis [24] and with the results of Schmidt et al. [4]. A satisfactory agreement is obtained. In general, the over-all level of matching of our static limit data with the previous fully-static results is a good check of the consistency of our starting point for further calculations.

Next we studied the influence of various ionic environments on the dynamic dipole polarizability of ions. In the region of our study, the anionic polarizabilities are particularly far more interesting than their cationic counterparts, and only their

Table 2. Static dipole polarizabilities (in $Å^3$) of cation and anion pairs – in-crystal values

Crystal	In-crystal pair polarizability	
	Present	Other values
LiF	0.950	0.915[a]
NaF	1.175	1.178[a], 1.180[b]
KF	1.985	1.992[a], 1.966[b]
LiCl	2.992	2.905[a]
NaCl	3.316	3.283[a], 3.134[b]
KCl	4.256	4.178[a], 4.002[b]

[a] Ref [24]
[b] Ref [4]

Table 3. In-crystal and vacuum (free) dynamic polarizability (in a.u.) of F^- in different environments as a function of the frequency ω (in a.u.) of the external driving field

	Dynamic polarizability of F^-					
ω	LiF	NaF	KF	RbF	CsF	Vacuum
0.0	6.22	6.97	7.77	8.14	8.50	10.56
0.02	6.23	6.98	7.78	8.16	8.51	10.59
0.04	6.25	7.01	7.82	8.20	8.56	10.70
0.06	6.28	7.05	7.88	8.27	8.64	10.89
0.08	6.33	7.12	7.96	8.37	8.75	11.18
0.10	6.39	7.20	8.08	8.50	8.91	11.59
0.12	6.46	7.31	8.23	8.68	9.11	12.20
0.14	6.56	7.44	8.42	8.90	9.37	13.13
0.16	6.67	7.60	8.66	9.18	9.70	14.77
0.18	6.81	7.81	8.95	9.54	10.1	20.32
0.1844						175.7
0.1845						− 673.3
0.19						21.06
0.20	6.98	8.05	9.33	10.0	10.7	
0.22	7.17	8.36	9.82	10.6	11.5	
0.24	7.42	8.75	10.5	11.5	12.6	
0.26	7.71	9.24	11.4	12.7	14.3	
0.28	8.09	9.91	12.8	14.7	17.5	
0.30	8.57	10.9	15.2	18.8	26.2	
0.32	9.21	12.3	20.7	33.2	283	
0.3213					10156	
0.3214					− 5702	
0.33				83.1	− 32.2	
0.3348				4893		
0.3349				− 13709		
0.34	10.1	15.0	53.6	− 60.7		
0.3476			154418			
0.3477			− 3470			
0.35			− 133			
0.36	11.6	21.7				
0.38	14.2	106				
0.3833		24678				
0.3834		− 3738				
0.39		− 40.2				
0.40	21.8					
0.42	1069					
0.4202	3792					
0.4203	− 13351					
0.43	− 22.5					

in-crystal and vacuum (free state) frequency-dependence are displayed in Tables 3 and 4. As can be seen from these tables, the polarizability initially remains almost constant at the zero-frequency value exhibiting only a small but monotonic increase that gradually culminates in a steep and enormous growth followed by a sudden discontinuity in its sign. Considering the frequency-dependence of the orbital polarizabilities separately, it was noticed that this jump is essentially due to

Table 4. In-crystal and vacuum (free) dynamic polarizability (in a.u.) of Cl^- in different environments as a function of the frequency ω (in a.u.) of the external driving field

	Dynamic polarizability of Cl^-					
ω	LiCl	NaCl	KCl	RbCl	CsCl	Vacuum
0.0	20.0	21.4	23.2	23.9	25.0	30.95
0.02	20.0	21.5	23.3	24.0	25.1	31.10
0.04	20.1	21.6	23.4	24.1	25.3	31.57
0.06	20.3	21.8	23.7	24.4	25.6	32.40
0.08	20.6	22.2	24.1	24.9	26.2	33.73
0.10	21.0	22.6	24.7	25.5	26.9	35.79
0.12	21.4	23.2	25.4	26.3	27.8	39.22
0.14	22.0	23.9	26.4	27.4	29.1	46.58
0.15						58.42
0.1566						1727
0.1567						− 1788
0.16						− 26.15
0.16	22.8	24.8	27.6	28.8	30.8	
0.18	23.7	26.0	29.3	30.7	33.2	
0.20	24.9	27.6	31.6	33.4	36.8	
0.22	26.5	29.8	34.9	37.6	42.9	
0.24	28.6	32.9	40.6	45.2	56.5	
0.26	31.7	38.0	52.7	65.8	142	
0.2666					83718	
0.2667					− 7925	
0.27				106	− 181	
0.2793				28465		
0.2794				− 9372		
0.28	36.8	48.9	118	− 1015		
0.2879			49504			
0.2880			− 8041			
0.29			− 301			
0.30	48.0	102				
0.3088		14443				
0.3089		− 11686				
0.31		− 529				
0.32	115					
0.3269	13281					
0.3270	− 11066					
0.33	− 168					

the predominating sharp rise of the $p \rightarrow s$ valence orbital contribution over others in approaching the region of discontinuity i.e. the pole. It owes its origin to the well-known divergence of the corresponding first-order perturbation amplitude at resonance in absence of any phenomenological damping term in the theory. In the immediate neighbourhood of a discontinuity, finer scanning is performed in order to pinpoint the pole. The present calculation is carried out upto the first poles encountered for F^- and Cl^- in different alkali halide environments, and the effect of environments is evident from the tabulated results. The position of the pole recedes to the lower frequencies as a particular anion combines with larger cations, (i.e. in a smaller Madelung potential) and also for larger anions with a particular

cation, as might be expected. Over the entire range upto and just beyond the first pole of an anion in its respective halides, a much slower and smooth variation of the polarizability with frequency is registered for different metal partners and consequently, these are not listed in the Tables (for example, the Li^+, Na^+ and F^+ polarizabilities grow approximately by 2.5%, 4.2% and 16.3% over their static values upto the poles for F^- in their respective fluorides, and by 1.5%, 2.5% and 9.6% upto to the poles for Cl^- in their chlorides).

The pole of the in-crystal anion polarizability represents an excitation and should be interpretable within the familiar absorption framework of the solid. For negative ions in their free states, the pole occurs at the absorption frequency of the lowest singly excited bound state embedded in the detachment continuum, which is characterised by the excitation energy (0.1844 a.u. for $2p^5 3s$: F^- and 0.1566 a.u. for $3p^5 4s$: Cl^- from our calculation) greater than the orbital ionization energy ($\varepsilon_{2p}^{HF} \approx 0.1808$ a.u. for F^- and $\varepsilon_{3p}^{HF} \approx 0.1499$ a.u. for Cl^-). The existence of such states has been reported in a number of earlier work [25–28] on negative ions. Under the influence of the crystal potential, however, the negative ion becomes much more bound; the orbital (and the total) energies are significantly lowered (for instance, $-\varepsilon_{2p}^{C}$ for F^- went down from -0.4767 a.u. in CsF to -0.5480 a.u. in LiF, while $-\varepsilon_{3p}^{C}$ for Cl^- reduced from -0.3986 a.u. in CsCl to -0.4646 in LiCl). So, relative to the bottom of the valence orbital, the ionization continuum is pushed up considerably such that the previously mentioned excitations of the anion may now occur well-below the continuum despite an increase in this transition energy for crystal-ions – as, for a particular anion, the transition energy (measured by the pole-position) goes up with smaller cations, at the same time the continuum is also pushed up further.

Now, it would be meaningful to relate the in-crystal poles of the anion polarizability to the crystal absorptions. We recall to the well-known fact that at the vacuum ultraviolet (vuv) absorption edges of alkali halide crystals, no photoconductivity (and so, no valence to conduction band transition) occurs and the onset of absorption is generally ascribed to excitonic transition below the conduction band. The current calculation (within its limited framework, ignoring spin–orbit effects) describes such a localized picture of electronic excitation centered on the halogen crystal-ion analogous to the excited state of an atom. Therefore, the first poles of the anion polarizability occurring in different crystalline environments may be identified as the simulation of the lowest exciton-like absorptions in alkali halide crystals by the model potential. In Table 5 we compare the computed pole-positions for F^- and Cl^- against the room-temperature experimental data [29–31] for the lowest-energy vuv-absorption peaks in their respective halides. A close correspondence is observed with these $n = 1$ excitonic transitions. In view of the simplicity of the model potential, it is indeed gratifying that a reasonable agreement (within 1.5–6.5%) in the location of the absorption peaks is obtained as well as the correct direction of shifting of these peaks (to the low energy sides for larger ions) is reproduced in both the halides. Besides, the Madelung-potential (at the anion site)-dependence of the calculated anionic transition energy in crystal environments, as depicted in Fig. 1, would be noteworthy. Since the Madelung potential is proportional to $1/a$ (a = lattice constant) and is set equal to V^C ($r \leqslant R$), Fig. 1 would also represent the variation of the anionic transition energy with the inverse of the Watson sphere radius R or lattice constant a. For both the anions F^- and Cl^-, it could be possible to obtain linear fits $y = a + bx$ to the computed in-crystal anionic transition energies or the pole-positions (y) in their respective halides as a function of the Madelung potentials (x) at the anion site,

Table 5. Comparison of the environment-dependent pole-positions (in eV) of the anion polarizability with the experimental vuv-absorption edges of alkali halide crystals

Anion	Crystal/ environment	Calculated location of the pole	Experimental vuv-absorption edge
	LiF	11.43	11.1 (?)[a]
	NaF	10.43	10.45[b], 10.6[c]
F^-	KF	9.46	9.80[b]
	RbF	9.11	9.30[b]
	CsF	8.74	9.13[b]
	Vacuum	5.02	
	LiCl	8.90	8.60[b]
	NaCl	8.40	7.85[a], 7.88[b]
Cl^-	KCl	7.83	7.70[a,b]
	RbCl	7.60	7.48[b]
	CsCl	7.25	7.40[b]
	Vacuum	4.26	

? There is some evidence for extrinsic absorption of unknown origin in the edge
[a] Ref 29
[b] Ref 31
[c] Ref 30

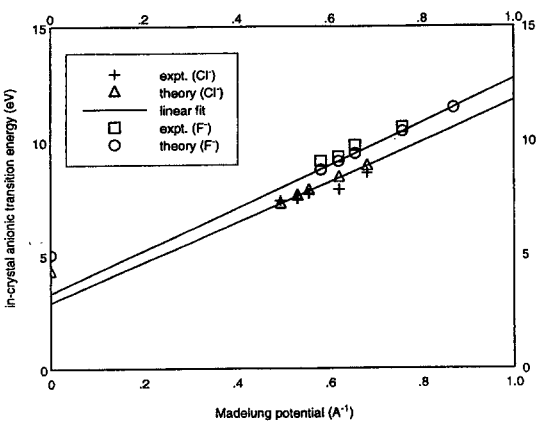

Fig. 1. Variation of the in-crystal anionic transition energy with the Madelung potential in alkali halides

with the following fitting parameters:

$$F^-: \quad a = 3.319, \; b = 9.371$$

$$Cl^-: \quad a = 2.905, \; b = 8.842$$

In the same graph the trends of the experimental values for these salts are also indicated.

In the preceding paragraphs we have seen the influence of crystal potential on the dispersion and absorption characteristics of anions and next we consider

Table 6. Crystal-potential-induced enhancement in the absorption oscillator strength (f) values and transition probabilities (in s^{-1}) of the lowest dipole transitions of anions and comparison against the f-values of the first excitonic transitions in alkali halides

Anion	Crystal/ environment	f values		Transition probability
		Present	$n = 1$ excitonic absorption	
F^-	LiF	0.248		1.40(9)*
	NaF	0.249		1.17(9)
	KF	0.236		9.11(8)
	RbF	0.241		8.65(8)
	CsF	0.235		7.74(8)
	Vacuum	0.005		5.59(6)
Cl^-	LiCl	0.395		1.35(9)
	NaCl	0.399	0.3–0.6[a], 0.2[b], 0.4[c]	1.22(9)
	KCl	0.398	0.3–0.6[a]	1.05(9)
	RbCl	0.394		9.82(8)
	CsCl	0.386		8.77(8)
	Vacuum	0.028		2.16(7)

[a, b] Ref 33 (derived from experimental data)
[c] Ref 33 (calculated from the excitation model)
* $m(n) = m \cdot 10^n$

how the transition amplitude is modified due to the presence of crystalline environments. We estimate the absorption oscillator strength (for the lowest dipole transition under consideration from the ground state of the anion) defined as (in the length form),

$$f_{mn} = (2/3)\omega_{mn} |\langle m|r|n\rangle|^2 \tag{9}$$

and derivable from the frequency-dependent dipole polarizability via the following standard relation [32]:

$$\alpha_d(\omega) = \sum_n{}' \frac{f_{mn}}{\omega_{mn}^2 - \omega^2} \tag{10}$$

where all the symbols are understood in their usual sense. At resonance the contribution from the corresponding transition becomes predominantly large and knowledge of the dispersion data in the close vicinity of the pole is required (normally upto the 4th decimal place of energy is seen to suffice). In Table 6 are presented the oscillator strengths evaluated for the lowest transitions of the anions in different crystalline environments. Earlier references to these strengths are rather sparse and also a certain amount of disagreement in them is documented in the literature. The value derived from the experimental data and from different theoretical models of the excitonic transition for the first vuv-absorption in pure alkali halide crystals differ considerably among themselves. The nearest-neighbour anion to cation charge-transfer model of the exciton predicts a value 1.585 for NaCl that is far too great with respect to the much smaller estimate 0.4 of Dexter [33] based on the localized excitation of the halogen ion model. Of the total oscillator strength (3.25: NaCl, 3.24: KCl and representing the sum for all excitations to the bound and continuum states) determined from an inspection of the relative absorption

curve and refractive index data, a fraction (1/5 to 1/10) has been attributed to the first exciton absorption leading to a recommended range (0.3–0.6) for this transition in NaCl and KCl [33]. Also in the same article it was shown that a somewhat different line of analysis of the experimental data would produce a value 0.2 of this strength. In our calculation we have observed that the estimated oscillator strengths for the lowest transition are very small for anions in their free-states: $f_{3p\to 4s} = 0.0275$ for Cl^- and $f_{2p\to 3s} = 0.051$ for F^-. But these are largely enhanced by an order of magnitude in the crystal potentials, as can be seen from Table 6 yielding approximately 0.40 and 0.25 for Cl^- and F^-, respectively. The exact agreement of the predicted strength for NaCl from this work with that of the excitation model is definitely somewhat fortuitous since actually only a small variation in the computed strengths is noticed in different fluoride and chloride environments (this is perhaps consistent if the near equality of the total strengths for NaCl and KCl, as mentioned earlier, is considered), with no clear manifestation of the nature of variation. In the estimated transition probabilities ($= 2\omega_{mn}^2 f_{mn}$), however, a downward trend with larger metal ions is apparent in both of the two halides because of its ω_{mn}^3 dependence.

In conclusion, adopting a time-dependent procedure combined with a simple model of the crystal potential, we have demonstrated in this calculation the influence of environments on linear response of ions under a time-dependent field. It is shown how the dispersion and pole position of the frequency-dependent dipole polarizability of anions are modified in accordance with the vuv-absorption edges attributed to excitonic transitions in alkali halide crystals. This is further confirmed by the supporting magnitude of the absorption oscillator strengths of these dipole transitions, estimated directly from the in-crystal dynamic polarizability. It appears that such an approach would be capable of simulating the structural details and multiplicity of localized electronic excitations in solids – intrinsic as well as impurity-induced, provided descriptions of the local ionic environment and the excited state are incorporated in addition to keeping an allowance in the method for treating the well-known spin–orbit splitting in the cases of excitons. From an accurate *ab initio* quantum chemical viewpoint, perhaps also worth-considering would be contribution of intra- and inter-ionic electron correlation to dynamic response and the properties derived therefrom, albeit much less prominent as one may expect for solids.

Acknowledgments. D.R. gratefully acknowledges the research fellowship granted to him by the Alexander von Humboldt-Stiftung. He is indebted to Prof. P.K. Mukherjee for encouragement and support.

References

1. Paschalis E, Weiss Alarich (1969) Theor Chim Acta 13:381
2. Schmidt PC, Weiss Alarich, Das TP (1979) Phys Rev B 19:5525
3. Schmidt PC, Sen KD, Das TP, Weiss Alarich (1980) Phys Rev B 22:4167
4. Schmidt PC, Sen KD, Weiss Alarich (1980) Ber Bunsen-Ges Phys Chem 84:1240
5. Maessen B, Schmidt PC (1981) Theor Chim Acta 59:299
6. Pearson EW, Jackson MD, Gordon RG (1984) J Phys Chem 88:119
7. Mahan GD (1980) Solid State Ionics 1:29
8. Fowler PW, Madden PA (1983) Mol Phys 49:913
9. Fowler PW, Madden PA (1984) Phys Rev B 29:1035
10. Fowler PW, Madden PA (1984) Phys Rev B 30:6131
11. Fowler PW, Madden PA (1985) J Phys Chem 89:2581

12. Fowler PW, Tole P (1988) Chem Phys Lett 149:273
13. Fowler PW, Tole P (1989) J Chem Soc Chem Comm 1652
14. Kelly HM, Fowler PW (1993) Mol Phys 80:135
15. Fowler PW, Kelly HM (1994) Z Naturforsch 49a:125
16. Fowler PW, Knowles PJ, Pyper NC (1985) Mol Phys 56:83
17. Fowler PW, Pyper NC (1986) Mol Phys 59:317
18. Watson RE (1958) Phys Rev 111:1108
19. Pitzer RM, Atomic self-consistent-field program by the basis set expansion method (Quantum Chemistry Program exchange, Program No. 587), Indiana University
20. Heinrichs J (1968) Phys Rev 172:1315
21. Langhoff PW, Epstein ST, Karplus M (1972) Rev Mod Phys 44:602
22. Löwdin PO, Mukherjee PK (1972) Chem Phys Lett 14:1
23. Coker H (1976) J Phys Chem 80:2078
24. Wilson JN, Curtis RM (1970) J Phys Chem 74:187
25. Fung AC, Matese JJ (1972) Phys Rev A 5:22
26. Bunge CF (1980) Phys Rev A 22:1
27. Canuto S, Duch W, Geersten J, Miller-Plathe F, Oddershede J, Scuseria G (1988) Chem Phys Lett 147:435
28. Das AK, Mukherjee PK (1993) Theor Chim Acta 85:371
29. Palik ED (ed) (1985) Handbook of optical constants of solids, vol I, Academic Press, New York
30. Palik ED (ed) (1991) Handbook of optical constants of solids, vol II, Academic Press, New York
31. Eby JE, Teegarden KJ, Dutton DB (1959) Phys Rev 116:1099
32. Sobelman II (1979) Atomic Spectra and Radiative Transitions. Springer, Berlin, Heidelberg, New York
33. Dexter DL (1957) Phys Rev 108:707